GROUND-BASED SPATIAL INTERFEROMETERS AND ATMOSPHERIC TURBULENCE

V.P. Lukin and B.V. Fortes

Institute of Atmospheric Optics,
Siberian Branch of the Russian Academy of Sciences, Tomsk
Received May 12, 1995

The asymptotic and numerical analysis of the phase difference spectrum for stellar interferometers has been performed based on the models of atmospheric turbulence. The influence of the outer scale of turbulence is studied. The results of field measurements carried out using stellar interferometers in different parts of the world, are analyzed using data available from literature.

1. INTRODUCTION

In recent years in some countries (USA, France, Germany, United Kingdom, Australia) the stellar optical interferometers with large measuring bases have been developed and designed. One of the first stellar interferometers using new technologies is the Mark II stellar interferometer with the measuring base of 31 m. The developed Mark III stellar interferometer (a modern type of the interferometers with the measuring base of 12 m oriented along the north-south direction) was used as a prototype of two big instruments for operating through the atmosphere in the Lowell Observatory, the vicinity of Flagstaff, Arizona, USA, namely the astronomical interferometer (AI) of the USA Naval Observatory and the Large Optical Antenna (LOA) of the Naval Research Observatory. The maximum measuring base in the Large Optical Antenna will be 473 m. The creation of these stellar optical interferometers has become possible because of new optical technologies, namely, laser systems providing maintenance of a constant spacing of the interferometer as well as for adopting the elements and systems of adaptive optics to suppress noise.

In parallel with these optical antenna arrays, large telescopes—interferometers have been designed. For example, at the Mauna Kea Observatory on the Hawaii the Kekk II telescope has being constructed, which, operating in pair with the Kekk telescope (the diameter of the main mirror 10 m), will form the optical interferometer with the base of 85 m.

The European Southern Observatory is conducting the construction (in Chile at the Sierra Paranal Observatory) of the Very Large Telescope—Interferometer (VLTI) consisting of four telescopes with the aperture 8.2 m in diameter. In this interferometer the maximum distance between the interfering optical beams (maximum base) is 128 m.

First of all, it should be noted that these new optical instruments will make it possible to conduct observations of stellar objects with the angular resolution better than 10^{-8}. These unique instruments,

operating through the atmosphere, will provide acquisition of very important information concerning the atmospheric structure in different parts of the world. In its turn, these instruments should be provided with reliable data on the state of the atmosphere.

2. ATMOSPHERIC EFFECTS

The effects of the atmosphere on the operation of ground—based optical interferometers has been studied quite intensively.[2–7] We would like to further investigate some problems first considered in Ref. 3. First of all, we shall consider the influence of atmospheric turbulence on the characteristics of telescope—interferometers with large optical bases. Although for a complete understanding of the influence of the atmosphere on the operation of a ground—based telescope we must consider the astronomical refraction and molecular absorption of radiation.

Undoubtedly the problem on estimating the phase fluctuation for interferometers with large optical bases is closely associated with the altitude variation of the turbulent state of the atmosphere. We mean here, in particular, the spectral density of the refractive index fluctuations of the atmosphere. We shall start off from the possibility of describing the atmospheric turbulence in the framework of models taking into account vertical profiles of the structure parameter of the refractive index of the atmosphere $C_n^2(h)$, altitude variations of the wind velocity vector $\mathbf{v}(h)$ and the value of the outer scale of turbulence $\varkappa_0^{-1}(h)$.

We assume in our calculations that the stellar radiation, as an unlimited plane wave, when propagating through the atmosphere, falls on two small apertures of the interferometer. To obtain high contrast of the interference pattern it is necessary to select the size of the receiving aperture to be less than the value r_0 of the Fried radius. The value of the error of astronomical measurements connected with the fluctuation of phase difference δs (on the interferometer base b) due to the influence of the atmospheric

turbulence is described[8] via the time spectral density of the phase difference fluctuations:

$$W_{\delta s}(f) = 16\,\pi k^2 \int\limits_0^L d\xi \iint d^2\varkappa\, \Phi_n(\varkappa,\,\xi)\times$$

$$\times[1 - \cos(\varkappa\,\mathbf{b})]\int\limits_0^\infty d\tau\,\cos(\varkappa\,\mathbf{v}\,\tau)\,\cos(2\,\pi\,f\,\tau)\,, \qquad (1)$$

where f is the frequency; ξ is the integration variable along the atmospheric path, $k = 2\pi/\lambda$ is the wave number of radiation, $\Phi_n(\varkappa,\xi)$ is the spectral density of the atmosphere refractive index fluctuations, $\mathbf{b}$ is the radius-vector characterizing the value and orientation of the interferometer base, $\mathbf{v}$ is the vector of wind velocity. In the below calculations we shall use the following property of the Dirac δ-function

$$\int\limits_0^\infty d\tau\,\cos(2\,\pi\,f\,\tau)\,\cos(\varkappa\,\mathbf{v}\,\tau) =$$

$$= \frac{\pi}{2}\,[\delta(2\pi f - \varkappa\,\mathbf{v}) + \delta(2\pi f + \varkappa\,\mathbf{v})]\,, \qquad (2)$$

and assume that the spectrum of $\Phi_n(\varkappa,\,\xi)$ is isotropic for all scales $|\varkappa|$ of turbulent inhomogeneities.

Let us introduce into the consideration the angle α between the vectors $\mathbf{v}$ and $\mathbf{b}$. Let the running angle between the vectors $\varkappa$ and $\mathbf{v}$ be designated by φ, then

$$\delta(\varkappa\,\mathbf{v} \pm 2\pi f) = (\varkappa\,v)^{-1}\,\delta(\cos\varphi \pm 2\pi f/\varkappa\,v)\,.$$

As a result we have the following expression

$$W_{\delta s}(f) = 32\,\pi^2\,k^2 \int\limits_0^L d\xi\,v^{-1}\times$$

$$\times \int\limits_0^\infty d\,u\,\Phi_n((u^2 + 4\,\pi^2 f^2/v^2)^{1/2},\,\xi)\times$$

$$\times\left[1 - \cos\!\left(\frac{2\pi f\,b}{v}\cos\alpha\right)\cos(bu\sin\alpha)\right], \qquad (3)$$

where $v = |\mathbf{v}|$, $\varkappa = |\varkappa|$, $b = |\mathbf{b}|$.

It is easy to show that the expression in brackets in Eq. (3) at $\mathbf{v}\!\uparrow\uparrow\,\mathbf{b}$ (when $\alpha = 0$) is reduced to $[1 - \cos(2\pi fb/v)]$ and to $[1 - \cos(bu)]$ at $\mathbf{v}\perp\mathbf{b}$ ($\alpha = \pi/2$).

It should be noted that the expression (1) is written in the geometric optics approximation, while smooth perturbation method[8] requires the introduction of the term $\cos^2(\varkappa^2(L - \xi)/2k)$ in the integrand.

3. ASYMPTOTIC ANALYSIS

The calculations of the spectral density of the phase difference fluctuations are carried out using the Karman model[9–12] of the atmospheric turbulence spectrum

$$\Phi_n(\varkappa,\,\xi) = 0.033\,C_n^2(\xi)\,(\varkappa^2 + \varkappa_0^2)^{-11/6}\,, \qquad (4)$$

where $C_n^2(\xi)$ and $\varkappa_0(\xi)$ are the parameters of the model. Thus we shall study the peculiarities of the $W_{\delta s}(f)$ spectrum behavior connected with the finite value of the outer scale of turbulence. By substituting the spectrum (4) to the expression (3) and after a series of calculations we obtain

$$\int\limits_0^\infty du\,\Phi_n((u^2 + 4\,\pi^2 f^2/v^2)^{1/2},\,\xi)\times$$

$$\times\left[1 - \cos\!\left(\frac{2\pi f\,b}{v}\cos\alpha\right)\cos(bu\sin\alpha)\right] =$$

$$= \frac{\Gamma(1/2)\,\Gamma(4/3)}{2\Gamma(11/6)}\,t^{-8/3}\left[1 - \cos\!\left(\frac{2\pi f\,b}{v}\cos\alpha\right)\times\right.$$

$$\times\left\{{}_1F_2\!\left(\frac{1}{2}\,;\,-\frac{1}{3}\,,\frac{1}{2}\,;\,\frac{t^2 b^2\sin^2\alpha}{4}\right) + \right.$$

$$+\, \Gamma(-4/3)\,\Gamma^{-1}(4/3)\left(\frac{b\,t\,\sin\alpha}{2}\right)^{8/3}\times$$

$$\left.\left.\times\,{}_1F_2\!\left(\frac{11}{6}\,;\,\frac{11}{6}\,,\frac{7}{3}\,;\,\frac{t^2 b^2\sin^2\alpha}{4}\right)\right\}\right], \qquad (5)$$

where $t^2 = \varkappa^2 + 4\pi^2 f^2/v^2$ and ${}_1F_2(\dots)$ is the Gauss hypergeometric function.

Using expressions (5) and (3) one can obtain the spectrum of phase difference at an arbitrary orientation of the vectors $\mathbf{v}$ and $\mathbf{b}$.

In the case of $\mathbf{v}\!\uparrow\uparrow\,\mathbf{b}$ we obtain

$$W_{\delta s}(f) = 0.065\,k^2\int\limits_0^L d\xi C_n^2\,v^{5/3}\,f^{-8/3}\times$$

$$\times\left[1 - \cos\!\left(\frac{2\pi f\,b}{v}\right)\right][1 + \varkappa_0^2\,v^2/4\pi^2\,f^2]^{-4/3}\,, \qquad (6)$$

what well agrees with the calculations in Ref. 3. Interferometers can be conditionally subdivided into "small" and "large" with respect to the relative value of the measuring base b. So, in the region of high frequencies ($f > v/b$) the expression (6) takes the form:

$$W_{\delta s}(f) = 0.065\,k^2\,f^{-8/3}\int\limits_0^L d\xi\times$$

$$\times C_n^2\,v^{5/3}\,[1 + \varkappa_0^2\,v^2/4\pi^2\,f^2]^{-4/3}\,, \qquad (7)$$

which results in

$$W_{\delta s}(f) \approx 0.065\,k^2\,f^{-8/3}\int\limits_0^L d\xi\,C_n^2\,v^{5/3}\,. \qquad (8)$$

for "small" interferometers ($\varkappa_0^{-1} > b$).

In the low-frequency range $(f < v/b)$,

$$W_{\delta s}(f) \approx 1.29\ k^2\ b^2\ f^{-2/3} \int\limits_0^L d\xi \times$$

$$\times\ C_n^2\ v^{-1/3}\ [1 + \varkappa_0^2\ v^2/4\pi^2\ f^2]^{-4/3}\ , \qquad (9)$$

for "small" interferometers $(b < \varkappa_0^{-1})$ the spectrum

$$W_{\delta s}(f) \approx 1.29\ k^2\ b^2\ f^{-2/3} \int\limits_0^L d\xi\ C_n^2\ v^{-1/3} \qquad (10)$$

keeps the power-law form, while if the interferometer is "large" (or $\varkappa_0^{-1}$ is comparable with b)

$$W_{\delta s}(f) \approx 174\ k^2\ b^2\ f^2 \int\limits_0^L d\xi\ C_n^2\ \varkappa_0^{-8/3}\ v^{-3}\ . \qquad (11)$$

Thus, the spectrum of phase difference fluctuations (at $\mathbf{b} \uparrow\uparrow \mathbf{v}$) for "large" interferometers can have singularities.

Now consider in move detail the opposite case $\mathbf{v} \perp \mathbf{b}$, $\alpha = \pi/2$ in Eqs. (3) and (5). In this case we have the following expression:

$$W_{\delta s}(f) = 16\ \pi^2\ k^2\ 0.033\ \frac{\Gamma(1/2)\ \Gamma(4/3)}{2\Gamma(11/6)} \times$$

$$\times \int\limits_0^L \frac{d\xi\ C_n^2}{v}\ t^{-8/3} \times \left[1 - \left\{ {}_1F_2\left(\frac{1}{2}\ ;\ -\frac{1}{3}\ ,\ \frac{1}{2}\ ;\ \frac{t^2\ b^2}{4}\right) + \right. \right.$$

$$\left. \left. + \frac{\Gamma(-4/3)}{\Gamma(4/3)}\left(\frac{b\ t}{2}\right)^{8/3}\left({}_1F_2\left(\frac{11}{6}\ ;\ \frac{7}{3}\ ,\ \frac{11}{6}\ ;\ \frac{t^2\ b^2}{4}\right)\right)\right\}\right]. \qquad (12)$$

We can consider the following asymptotic form of the Eq. (12) when

$$b\ t = (\varkappa_0^2\ v^2 + 4\pi^2\ f^2\ b^2/v^2) \ll 1\ , \qquad (13)$$

i.e., simultaneously at low frequencies and $\varkappa_0^{-1} > b$, so we have

$$W_{\delta s}(f) \approx 6.58\ k^2\ b^2 \int\limits_0^L d\xi\ C_n^2\ v^{-1}\ (\varkappa_0^2 + 4\pi^2 f^2/v^2)^{-1/3}\ .$$

$$\qquad (14)$$

Two limiting cases are possible in Eq. (14):

$$W_{\delta s}(f) \approx 6.58\ k^2\ b^2 \int\limits_0^L d\xi\ C_n^2\ v^{-1}\ \varkappa_0^{-2/3} \qquad (15)$$

at $4\pi^2 f^2 \ll \varkappa_0^2\ v^2$,

$$W_{\delta s}(f) \approx 1.96\ k^2\ b^2\ f^{-2/3} \int\limits_0^L d\xi\ C_n^2\ v^{-1/3} \qquad (16)$$

at $4\pi^2 f^2 \gg \varkappa_0^2\ v^2$.

For the arbitrary values of f/v and $\varkappa_0^{-1}$ it is necessary to use Eq. (14), which exists only in the case when $\varkappa_0 b \ll 1$.

If $\varkappa_0^{-1} \sim b$ (we have the case of "large" interferometers) then Eq. (12) has no a low-frequency asymptotics of the type (14).

Under conditions $4\pi^2 f^2 \ll \varkappa_0^2 v^2$ but $b > \varkappa_0^{-1}$, the argument in Eq. (12) is $bt = \varkappa_0 b$, and we obtain

$$W_{\delta s}(f) \approx 8.78\ k^2 \int\limits_0^L d\xi\ v^{-1}\ C_n^2(\xi) \times$$

$$\times\ (\varkappa_0^2 + 4\pi^2 f^2/v^2)^{-4/3}\left[1 - \left\{ {}_1F_2\left(\frac{1}{2}\ ;\ -\frac{1}{3}\ ,\ \frac{1}{2}\ ;\ \frac{\varkappa_0^2\ b^2}{4}\right) + \right. \right.$$

$$\left. \left. + \frac{\Gamma(-4/3)}{\Gamma(4/3)}\left(\frac{\varkappa_0\ b}{2}\right)^{8/3}\left({}_1F_2\left(\frac{11}{6}\ ;\ \frac{11}{6}\ ,\ \frac{7}{3}\ ;\ \frac{\varkappa_0^2\ b^2}{4}\right)\right)\right\}\right]. \quad (17)$$

As is seen from this expression, the value $W_{\delta s}$ is practically independent of frequency in the low frequency range $(f \ll \varkappa_0 v)$ if $\varkappa_0 b > 1$.

In the high frequency range $(f \gg v/b)$ there is no difference in the behavior of the phase difference spectrum (12) both for "small" and "large" interferometers.

4. ALTITUDE MODELS OF ATMOSPHERIC TURBULENCE

Only for homogeneous optical paths the above asymptotic analysis can define whether is the interferometer "large" or "small", i.e., when $C_n^2(\xi) = C_n^2(0)$, $\varkappa_0^{-1}(\xi) = \varkappa_0^{-1}(0)$, $v(\xi) = v(0)$.

To describe the optical radiation propagation along vertical and slant optical paths, one should use Eqs. (3), (5), (6), and (12), considering that the integration variables along a propagation path are:

— intensity of turbulence $C_n^2(\xi)$,

— the absolute value of wind velocity $v(\xi)$,

— the value of the outer scale of turbulence $\varkappa_0^{-1}(\xi)$

— the angle α between the vectors $\mathbf{v}$ and $\mathbf{b}$, that corresponds to the wind turn.

However, since all these values depend not simply on the altitude but on the altitude above the sea level, the possible variations of the model should be seriously discussed from this point of view (model parameters) depending on aerography of the underlying surface.

When calculating the phase fluctuations in the stellar interferometer, the following substitution

$$\int\limits_0^L d\xi(...) \Rightarrow \int\limits_{H_0}^\infty dh(...)$$

should be made in Eqs. (3),(5),(6),(12), where h is the running altitude, H_0 is the altitude at which the interferometer receiving apertures are located over the underlying surface.

When analyzing the spectra of phase difference in large interferometers based on the numerical calculations by Eqs. (3) or (5), we must pay attention to the altitude models of the turbulent atmosphere. As concerning the choice of $C_n^2(h)$ models no variations in the models used is known from literature.[12-17] Most vast material is available on the integral value of the turbulence intensity along vertical paths

$$\int\limits_{H_0}^{\infty} \mathrm{d}h \; C_n^2(h) \; ,$$

characterizing the size of the coherent part of the aperture (Fried's radius r_0) for different regions of the world. Models of the altitude C_n^2 profile are also numerous.[12-17] There is a lack of information on the direct consideration of the underlying surface effect on the model variations.[10-12]

At the same time, sceptical attitude should be noted to the models of the atmospheric turbulence spectrum when considering the finiteness of the outer scale of turbulence and, especially, the running value of this parameter for vertical paths.[18] For homogeneous near-ground paths it is shown that the value $\varkappa_0^{-1}$ is finite (comparable with the height above the underlying surface).[9,12] In this case, for astronomical observations a number of researchers[3-5] consider that the value $\varkappa_0^{-1}$ varies from hundreds of meters up to some kilometers.

At the same time, there are many observations whose results correspond to the values of the outer scale of the order of one meter.[2,11,18,20,21]

Undoubtedly, the outer scale of the turbulence undergoes serious variations both in the surface layer[9,10] and at large altitudes.[13-15] Therefore the outer scale of turbulence cannot be considered as a fixed value for the entire atmosphere. Let us consider some scenarios of the outer scale variations with the altitude:

$$\varkappa_0^{-1}(h) \approx 0.4 \; h \; , \tag{18a}$$

$$\varkappa_0^{-1}(h) = \begin{cases} 0.4 \; h & h \le 25 \text{ m} \\ 2 \sqrt{h} & h > 25 \text{ m} \; , \end{cases} \tag{18b}$$

$$\varkappa_0^{-1}(h) = \begin{cases} 0.4 \; h & h \le 25 \text{ m} \\ 2 \sqrt{h} & 25 \text{ м} < h \le 2000 \text{ m} \\ 88.4 \text{ m} & h > 2000 \text{ m} \end{cases} \tag{18c}$$

$$\varkappa_0^{-1}(h) = 4/[1 + ((h - 8500)/2500)^2] \; , \tag{18d}$$

$$\varkappa_0^{-1}(h) = 5/[1 + ((h - 7500)/2500)^2] \; . \tag{18e}$$

The model (18a) is recommended in Ref. 8 for small altitudes, the model (18b) has been proposed by D. Fried,[12] the model (18c) is a generalization of the first two models. The models (18d) and (18e) were

obtained as a generalization of the results of direct measurements in the USA, France, and Chile.[12-14] Similar values of this parameter have been obtained at the Mauna Kea observatory (Hawaii).[15] Some investigators have cast doubt on these models,[18,12] however, the altitude variations of the outer scale within a wide range have gained recognition what is quite justifiable instead of assigning some particular value to this parameter along an inhomogeneous path.

Of course the altitude variations of wind velocity vector are also important,[19] that is, both its absolute value and the angle α (between **v** and **b**). In our calculations we use the generalization of the measurements results[14-15] on the wind velocity.

As the asymptotic analysis carried out in Section 3 shows, different portions of the phase difference spectrum have different altitude behavior.

The model described in Ref. 17 is used as a model of altitude variations. To construct it, we used experimental data obtained above the ground with a smooth relief and the altitude of underlying surface above sea level about 2 km. Then the two envelope curves have been drawn, one of them over the least values of C_n^2 observed. These values imply the best conditions for light propagation. Another curve envelopes the maximum C_n^2 values, i.e., the poorest propagation conditions. To characterize the intermediate conditions of propagation, the third profile was constructed as the average value of the first two ones.

5. DISCUSSION OF THE RESULTS

Our software[22] makes it possible to use effectively the whole set of models of the outer scale, turbulence intensity, and wind velocity. Among the parameters of the problem are the initial altitude H_0 and the value of the interferometer base as well as the angle α determining the orientation of the interferometer base. The calculations have been performed for the following interferometer bases: 3.1 m, 12 m, 36 m, 85 m, 128 m, 437 m, covering practically the entire range of operating and designed instruments. For convenience one diagram presents simultaneously three spectra of the phase difference fluctuations, namely, that at $\alpha = 0°$ (**v** ↑↑ **b**), $\alpha = 90°$(**v** ⊥ **b**), and at an arbitrary value of the angle α. The results of calculations are depicted in Figs. 1—4.

For the bases of 3.1 m and 12 m the calculations were made using different models of the outer scale of turbulence (see Figs. 1—2). These numerical calculations, as a whole, confirm the results of our asymptotic analysis: most variable is the phase difference spectrum at the interferometer orientation along wind (when the angle $\alpha = 0°$) in the low frequency range. At the same time, for the transverse orientation of the interferometer ($\alpha = 90°$) we observe practically indifferent spectral behavior in the low-frequency range. The high-frequency parts of these spectra are identical.
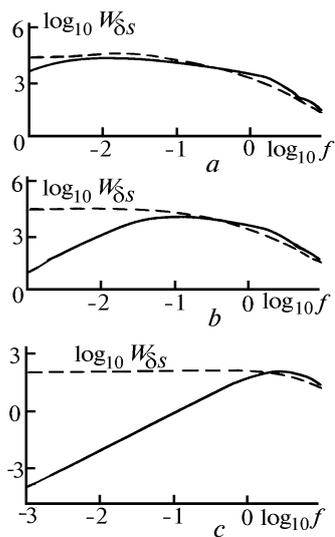
FIG. 1. The phase difference fluctuation spectra for the interferometer with the base 3.1 m. The turbulence profile corresponds to the medium conditions[17] of optical waves propagation in the atmosphere. Solid curves show spectra calculated for the case of the interferometer base being parallel to wind vector, dashed curves present the case of base being perpendicular to the wind velocity vector. The outer scale models (18a) (a), (18b) (b), and (18c) (c) have been used in calculations.
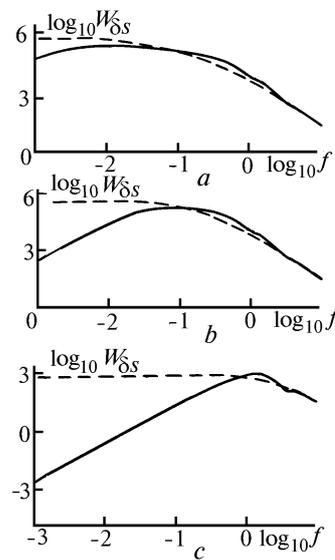
FIG. 2. The same as in Fig. 1 but for the interferometer with the base of 12 m.

It turned out that for all the models of altitude variation of the outer scale used one can select the averaged over the atmosphere value of the outer scale strongly affecting an optical characteristic measured. Practically for all models of the outer scale and turbulence intensity this value does not exceed 2 −5 m.
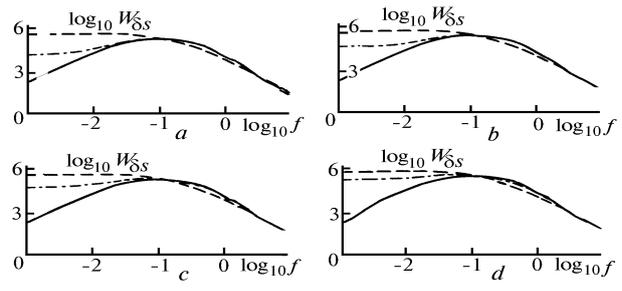
FIG. 3. The spectrum of phase difference fluctuations for the interferometer with the base of 12 m. The profile of turbulence is mean.[17] The model (18b) of the outer scale is used. Solid, dashed, and dot-and-dash curves show the spectra at parallel, perpendicular orientations of the base relative to wind velocity and at the values of the angle α = 10° (a), 15° (b), 20° (c), 30° (d).

Dependence of the phase difference spectrum on the value of the angle α (the angle between the vectors **v** and **b**) is also of interest. Figure 3 shows the results of calculations at different values of the angle α: 10, 15, 20, 30°. Numerical calculations show that already at the angle α exceeding 20° the phase difference spectrum corresponds practically to the spectrum $W_{\delta s}(f, 90°)$, i.e., when **v** ⊥ **b**.

In our opinion, the results from Refs. 3−5, where the phase difference spectrum has only two parts with the power-law dependences, $f^{-2/3}$ and $f^{-8/3}$, correspond mostly to the phase difference spectrum at **v** ⊥ **b**, i.e., at α = 90°.
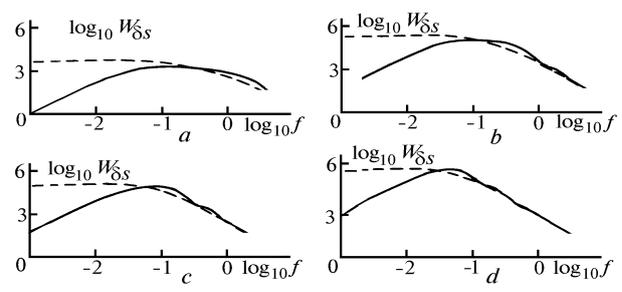
FIG. 4. The spectrum of phase difference fluctuations for the interferometer with the base of 3 (a), 12 (b), 33 (c), and 85 m (d). The profile of turbulence is of the best type.[17] The model (18b) of the outer scale is used. Solid and dashed lines show the spectra at parallel and perpendicular orientations of the base with respect to wind velocity.

We have investigated the variability of the phase difference spectra for different bases of interferometers: 3, 12, 38, and 85 m. Figure 4 shows that the increase of the interferometer base results in significant variations

of the phase difference spectrum (at $\alpha = 0°$). As the asymptotic analysis, these results point to the presence of parts where the spectrum varies proportionally to f^2, f^0, and $f^{-1/3}$.

Thus, so that the results of measurements of phase difference fluctuations, such as in Refs. 3—5, 20, and 21, will become a basis for improving models of turbulent atmosphere, it is necessary to fix, in measurements, the following parameters: initial altitude, the value and direction of wind velocity relative to the orientation of the interferometer base, the value of C_n^2 at the initial altitude, as well as the value of the contrast of interference fringes (for estimating the Fried radius value at the light wavelength used).

It should be noted, as a whole, that the predicting of the operation efficiency of large interferometers and modern telescopes, including those with adaptive optics, requires careful study of the influence of the atmosphere on the optical radiation propagation.

ACKNOWLEDGEMENT

REFERENCES

1. J. B. Breckinridge, ed.,B*Amplitude and intensity spatial interferometry II*,B Proc. SPIE **2200** (1994).
2. J.M. Mariotti and G.P. Di Benedetto, in: I.*A.U.Coloq. 79*, Garching, Apr. 9—12, 1984.
3. M. Colavita, M. Shao, and D.H. Staelin, Appl. Opt. **26**, No 19, 4106—4112 (1987).
4. D.F. Bucher, Proc. SPIE **2200**, 260—271 (1994).
5. C.A. Haniff, J.E. Baldwin and P.J. Warner, Proc. SPIE **2200**, 407—417 (1994).
6. B. Lopez and M. Sarazin, "*Optimum exposure times for interferometry*,B Technical Preprint No 36, European Southern Observatory, November 1991.
7. L.W. Bradford and S.M Flatte, Proc. SPIE **2200**, 396—406 (1994).
8. V.I. Tatarskii, *Wave Propagation in a Turbulent Medium* (McGraw - Hill, New York, 1961).
9. V.P. Lukin and V.V. Pokasov, Appl.Opt. **20**, No. 1, 121—135 (1981).
10. V.P. Lukin, Proc. SPIE **2200**, 384—395 (1994).
11. S.M. Gubkin, O.N. Emaleev, and V.P. Lukin, Astron. Journ. **69**, No. 4, 790—795 (1983).
12. R.E. Good, R.R. Beland, E.A. Murphy, J.H. Brown, and E.M. Dewan, Proc.SPIE **928**, 165—186 (1988).
13. C.E. Coulman, J. Vernin, Y. Coquenghiot, and J.L. Caccia, Appl.Opt. **27**, No. 1, 155—160 (1988).
14. B*Site Testing for the VLT. Data analysis*,B Part I, VLT Report No. 55, European Southern Observatory, 1987.
15. B*Site Testing for the VLT. Data analysis*,B Part I, VLT Report No. 60, European Southern Observatory, 1987.
16. V.P. Lukin, Atmos.Oceanic.Opt. **5**, No. 4, 229—242 (1992).
17. M.E. Gracheva and A.S. Gurvich, Izv. Akad. Nauk SSSR, Fiz. Atmos. Okeana **16**, No. 10, 1107—1111 (1980).
18. T.S. McKecnie, J.Opt. Soc. Am. A. **9**, No. 11, 1937—1954 (1992).
19. F. Murtagh and M.Sarazin, Scientific Preprint No. 934, European Southern Observatory, August 1993.
20. A. Sivaramakrishnan, R.J. Weyman, and J.W. Beletic, ESO Conference and Workshop Proceedings, No. 48, 9—14 (1993).
21. N. Takato, M. Iye, and I. Yamaguchi, ESO Conference and Workshop Proceedings, No. 48, 15—20, (1993).
22. B.V. Fortes and V.P. Lukin, Proc. SPIE **1668**, 477—488 (1992).